LAWRENCE
LIVERMORE
NATIONAL
LABORATORY

LLNL-JRNL-459996

Confirmation of Sampe Quality: XPS and UPS of UO2a

S. W. Yu, J. G. Tobin

October 15, 2010

Journal of Vacuum Science and Technology A

Disclaimer

Confirmation of Sample Quality: XPS and UPS of UO_2[a]

S.-W. Yu and J.G. Tobin[b,c]

Lawrence Livermore National Laboratory, LLNS-LLC, Livermore, CA

a)This article is based on material to be presented at the 57th Symposium of the American Vacuum Society: Abstract AC3+SS 202, AC+MI-TuM12.

b)American Vacuum Society member

c)Corresponding Author, Tobin1@LLNL.Gov

Abstract:

X-ray Photoelectron Spectroscopy (XPS) and Ultraviolet Photoelectron Spectroscopy (UPS) have been utilized to demonstrate the sample quality of a UO_2 specimen. This specimen is to be used in further studies with Bremstrahlung Isochromat Spectroscopy (BIS) and Fano Spectroscopy.

Materials terms: Uranium, Oxygen, Photoelectron Spectroscopy

Confirmation of Sample Quality: XPS and UPS of UO_2[a]

I. Introduction and motivation

Uranium dioxide (UO_2) is an important material, widely used as a fuel in nuclear reactors for the generation of electrical power. [1,2] Uranium and its compounds have been used to color ceramics, glass and even dentures. [3] More importantly for this study, uranium dioxide is a stable 5f material, that can serve as a low-radioactivity surrogate for more highly radioactive and chemically unstable materials such as Pu. This is particularly true if depleted Uranium is used, i.e. using low radioactivity isotopes of Uranium. Thus, uranium dioxide can serve as an appropriate material for the commissioning and testing of our new BIS/FANO Spectrometer. Here, BIS is Bremstrahlung Isochromat Spectroscopy, a high-energy variant of Inverse Photoelectron Spectroscopy (IPES) [4]. Fano Spectroscopy [5] is a type of photoelectron spectroscopy (PES), where chirally specific excitation and electron spin detection are applied to "non-magnetic" samples, that is materials without long range magnetic ordering such as in ferromagnetism or anti-ferromagnetism. Before this commissioning can proceed, it is essential that the sample quality of the uranium dioxide be established. To this end, an extensive study has been performed, using X-ray Photoelectron Spectroscopy (hv = 1487 eV from un-monochromatized AlK-alpha radiation and hv = 1254 eV from un-monochromatized MgK-alpha radiation [6]) and Ultraviolet Photoelectron Spectroscopy (hv = 21.2 eV from un-monochromatized HeI and hv = 40.8 eV from un-monochromatized HeII [7]). In this article, the results of this study will be presented, confirming the quality of the UO_2 specimen.

Before proceeding to a discussion of the XPS and UPS results for UO_2, it would be useful to briefly consider the spectrometer design and earlier results upon non-5f

systems, as well as the ultimate goal of these studies. Shown in Figure 1 is a schematic of the new Actinide Spectrometer [8,9] at LLNL. It includes unmonochromatized ultraviolet (UV) and X-ray sources and a photoelectron energy analyzer, all for Photoelectron Spectroscopy (PES). This photoelectron spectrometer has both a multi-channel, spin-integrated detector, located in the exit plane of the hemisphere, as well as a spin-specific mini-Mott detector. The Inverse Photoelectron Spectroscopy (IPES) or BIS measurements are performed using a photon monochromator system that includes multiple gratings and multichannel detection, plus a simple electron gun for excitation. Also presented in Figure 1 are some of our preliminary results for non-5f systems. The Fano Spectroscopy of platinum is shown, demonstrating the spin dependence of a valence band with a strong spin-orbit splitting and the absence of long-range magnetic ordering. [10, 11] Similarly, Ce Oxide has been probed with BIS/IPES, exhibiting very strong resonant behavior at the Ce3d threshold. [12] Ultimately, the objective of this project is to resolve the ongoing controversy of Actinide 5f electronic structure in general and Pu in particular, determining the nature of electron correlation in Pu. In Figure 1, the prediction of the Fano Spectroscopy result for Pu from one possible model is also illustrated. [11] It is experimental results, corresponding to such simulated predictions, which will ultimately solve the riddle of Pu electronic structure. [13]

II . Experimental

The experiments were performed in a combined BIS/Fano Spectrometer at LLNL [8,9] A schematic of the BIS/Fano capabilities can be found in Figure 1. The UO_2 was formed in the following manner: by polishing a Uranium sample and exposing it to air at ambient pressure and room temperature. After introduction into the vacuum system, the

sample of exposed uranium was prepared further by argon ion etching and mild heat treatment. The base pressure for the XPS/UPS measurements was 2 x 10^{-10} torr. In the XPS experiments, a Pass Energy of 25 eV was used in the Photoelectron Energy Analyzer and a total instrumental resolution band-pass of 2 eV was observed, based upon the full-width-at-half-maximum of the O1s core level peak, as described below. In the UPS experiments, a Pass Energy of 7 eV was used in the Photoelectron Energy Analyzer and an total instrumental resolution band-pass of 0.3 eV was observed, based upon the 10%-90% width of the Fermi Edge of a metallic sample. The other details of the UPS and XPS measurements will be described below. Unless otherwise specified, all measurements were made at normal emission and at or near room temperature.

III. Discussion of Spectral Results

A Elemental Sample Composition From XPS

Sample composition was determined using wide-scan XPS with both hv = 1487 eV (AlK-alpha) and hv = 1254 eV (MgK-alpha). The results of these measurements are shown in Figure 2. To facilitate direct comparison of the AlK-alpha and MgK-alpha spectra, the spectral intensities were plotted versus binding energy, using a spectrometer work function of 4 eV. In photoelectron spectroscopy, the following relation applies.

$$BE = hv - KE_{SP} - \phi_{SP} \qquad \text{Eq 1}$$

BE is binding energy. hv is the photon energy. KE_{SP} is the kinetic energy relative to the spectrometer zero or grounding and ϕ_{SP} is the spectrometer work function. For the XPS source, $\phi_{SP}^{XPS} = 4$ eV. Thus, for AlK-alpha, $BE_{Al} = 1483 - KE_{SP}$ and for MgK-alpha, $BE_{Mg} = 1250 - KE_{SP}$. The corresponding KE scales are shown in each panel.

Confirmation of Sample Quality: XPS and UPS of UO_2[a]

Only features associated with uranium or oxygen are observed: U5d (BE = ~ 100 eV), U5$p_{3/2}$ (BE = ~200 eV), U4f (BE = ~380, 391 eV) O1s (BE = ~530 eV), U4d (BE = ~740, 782), Oxygen Auger peaks (near KE = ~ 500 eV), U4$p_{3/2}$ (BE = ~ 1040 eV) and U NOV Auger (KE = ~ 200 eV). There is a weak feature at BE = ~350 eV, using AlK-alpha, but something like it is also observable in the U metal reference spectra. [6] Thus, this weak feature also appears to have its origin in U. In general, core levels such as the U4f and O1s appear at fixed binding energies and Auger peaks are seen at fixed kinetic energies. [4] For U, almost all of the core level peaks are spin-orbit split doublets. Within these constraints, the MgK-alpha and AlK-alpha spectra are in agreement. Furthermore, the different KE's of the AlK-alpha and MgK-alpha measurements suggest that there is not any variation of the result with depth. This is because the sampling depth in XPS is sensitive to the KE of the photoelectrons. [4] Hence, within the caveat of excitation cross-sections, it is clear that this sample is composed of only uranium and oxygen. In fact, the U peaks of the UO_2 sample are very similar in intensity and appearance to those in the metallic uranium calibration spectra, [6] for both the AlK-alpha and MgK-alpha excitations, respectively. The oxygen peaks exhibit similar agreement with those in the oxygen calibration spectra. [6] Having established that the sample is composed of only oxygen and uranium, the core levels of the uranium and oxygen will be considered in more detail, to quantify concentrations and robustness.

B Sample Stoichiometry and Stability from Core Level XPS

The U4f (Figure 3), O1s (Figure 4) and U4d (Figure 5), will be examined more carefully, using both AlK-alpha and MgK-alpha. These will be compared to chemically specific reference spectra, from various compounds. [14]

Confirmation of Sample Quality: XPS and UPS of UO_2[a]

For the U4f, both the AlK-alpha and MgK-alpha spectra exhibit the main spin-orbit split peaks at BE = 380 eV and 391 eV. Moreover, there are the satellite peaks (the "6 eV" satellites) at BE = 386 and 397 eV, associated with UO_2. [14, 15] Indeed, the spectra in Figure 3 are not only essentially identical to each other, but also the UO_2 reference spectrum in Reference 14 and 15, if broadening associated with instrumental resolution is taken into account. (It should be noted that elemental U has no "6 eV" satellites in the U4f spectrum. [14])

One way to address the instrumental resolution issue is to look at spectral structure without spin-orbit splitting or satellites. This has been done, using the O1s peak, shown in Figure 4. For Both AlK-alpha and MgK-alpha, there is a single peak, with a full-width-at-half-maximum of about 2 eV. This is substantially broader than the single O1s peak of Reference 15, where a higher resolution scan of UO_2 was performed, using monochromatized AlK-alpha radiation. However, the agreement in terms of binding energy is very good, indicating a consistency between the samples. From this measurement, an instrumental resolution band-pass of 2 eV is established for the XPS part of this study.

Finally, before moving on to a discussion of the valence band results, it is useful to consider the U4d spectral structure in Figure 5. Here, there are differences between the spectra for AlK-alpha and MgK-alpha radiation. However, this is not a sampling depth issue but instead is caused by the oxygen Auger features near KE = 500 eV. In the MgK-alpha spectrum, these overlap with the $U4d_{5/2}$ peak. Nevertheless, the $U4d_{3/2}$ peaks for both the AK-alpha and MgK-alpha are essentially identical. Furthermore, the AlK-alpha spectrum in Figure 5 can be compared to the reference spectra for UO_2 and

elemental uranium. [14,16] The spectrum in this study, with its peak/shoulder combination for both the U4$d_{5/2}$ and U4$d_{3/2}$, is consistent with the UO_2 reference spectrum and not with the elemental uranium. [14,16]

Again, the agreement between the AlK-alpha and MgK-alpha spectra for the U4f, O1s and U4d core levels suggests the absence of a sampling depth effect. Furthermore, the spectra in Figures 3, 4 and 5 at different times strongly suggests a temporal stability for the sample. Perhaps most importantly, the data in Figures 3, 4 and 5 all indicate that the sample is UO_2, not some other stoichiometry.

C Sample Stoichiometry: Valence Bands from XPS and UPS

The valence bands were probed with AlK-alpha, MgK-alpha, HeII and HeI radiation. (Figure 6) All of the results point to UO_2, without any indication of a second site or second structure.

Consider first the AlK-alpha and MgK-alpha spectra in Figure 6. Consistent with the core level data and wide-scans, the AlK-alpha and MgK-alpha valence band spectra are essentially identical and exhibit temporal stability over the time span that was tested. The XPS spectra are essentially identical with the valence band reference spectra. [14,17] This, in turn, leads to the peak assignments shown in the lower half of Figure 6.

Moreover, it is known [14,18] that the relative magnitude, of the U5f (BE = ~ 2 eV) and O2p (BE = ~ 6 eV), depends very strongly upon the oxygen stoichiometry (x) for UO_x. For UO_2, the U5f dominates the O2p. For UO_3, the U5f is almost completely gone, leaving the O2p as the dominant peak. The intervening stoichiometries, U_4O_9 (or $UO_{2.25}$) and U_3O_8 (or $UO_{2.67}$), show behavior between these extremes. The U_4O_9 has U5f and O2p peak heights that are almost the same, while the U_3O_8 has a U5f height that is less

than that of the O2p. This is further evidence that the sample is truly UO_2. If the oxygen concentration were to increase, the U5f/O2p peak ratio would drop precipitously, which would be inconsistent with out XPS measurements. Thus, there is only one site or structure and it is UO_2.

The UPS valence bands provide the two last pieces of evidence that the sample is UO_2. Shown in the upper half of Figure 6, the spectrum with KE between 12 eV and 44 eV includes both the stronger HeI and weaker HeII features. In the inset, an enhanced HeII spectrum is plotted. For HeI and HeII measurements, the spectrometer work function is $\phi_{SP}^{UPS} = 0$ eV. (The $\phi_{SP}^{UPS} = 0$ eV was determined using a conducting sample with a Fermi Edge and is the same for HeI and HeII.) Different spectrometer work functions, for the XPS source and the UPS source, are not unexpected. In the UPS data collection, the total resolution band-pass is much smaller, owing to lower analyzer pass energy and the narrower photon source widths. Because of this, it is possible to see more detailed spectral structure. For example, the band gap between the U5f peak and the Fermi Level (E_F) can be seen in Figure 6, for both HeI and HeII. Moreover, the HeI and HeII spectra are different: The U5f peak is stronger and the O2p peak has a bigger shoulder in HeII. The increase in the U5f intensity is due to an increase in the U5f cross-section in the range of hv = 20 to 40 eV. [19] These differences have been observed before. [14, 20,21] Respectively, the HeI and HeII spectra here are essentially identical to the earlier HeI and HeII spectra from UO_2. [14,20,21]

IV. Conclusions

Using XPS and UPS, and comparing to earlier calibration and reference spectra, it has been demonstrated that the sample is UO_2. This is without any discernable

contributions from a second site or second structure and without any variation of stoichiometry from the 1:2 ratio.

Acknowledgments

Lawrence Livermore National Laboratory is operated by Lawrence Livermore National Security, LLC, for the U.S. Department of Energy, National Nuclear Security Administration under Contract DE-AC52-07NA27344. This work was supported by the DOE Office of Science, Office of Basic Energy Science, Division of Materials Science and Engineering. The authors also wish to thank BW Chung and GD Waddill for their help on this project.

Confirmation of Sample Quality: XPS and UPS of UO_2[a]

References

1. Y. Guerin, G.S. Was, and S.J. Zinkle, MRS Bulletin **34**, 10 (2009).
2. F. Gupta, A. Pasterel and G. Brillant, Phys. Rev. B 81, 014110 (2010).
3. M. Betti, J. Environmental Radioactivity **64**, 113 (2003).
4. J.G. Tobin, "Photoemission and Inverse Photoemission," in "Determination of Optical Properties," Vol. VIII in Physical Methods of Chemistry, 2nd edition, Ed. B.W. Rossiter and R.C. Bretzold, John Wiley and Sons, New York, 1993, and references therein.
5. (A)U. Fano, Phys. Rev. **178**, 131 (1969); (B)U. Heinzmann, J. Kessler, and J.Lorenz, Phys. Rev. Lett. 25, 1325 (1970); (C)J.G. Tobin, S.W. Yu, T. Komesu, B.W. Chung, S.A. Morton, and G.D. Waddill, EuroPhysics Letters **77**, 17004 (2007); (D)S.W. Yu, T. Komesu, B.W. Chung, G.D. Waddill, S.A. Morton, and J.G. Tobin, Phys. Rev. B **73**, 075116 (2006); and references therein.
6. "X-ray Photoelectron Spectra," Physical Electronics Handbook, Eden Prairie, MN.
7. J.A.R. Samson, "Techniques of Vacuum Ultraviolet Spectroscopy," Wiley, New York, 1967.
8. J.G. Tobin, S.-W. Yu, B.W. Chung, G.D. Waddill and AL Kutepov, "Narrowing the Range of Possible Solutions to the Pu Electronic Structure Problem: Developing a new Bremstrahlung Isochromat Spectroscopy Capability," IOP Conf. Series: Materials Science and Engineering **9** (2010) 012054 doi:10.1088/1757-899X/9/1/012054.

9. S.W. Yu, B.W. Chung, J.G. Tobin T. Komesu, and G.D. Waddill, Nuclear Instr. Meth. Phys. Res. **A 614**,145 (2010).
10. S.W. Yu and J.G. Tobin, Surface Science Letters **601**, L127 (2007); S.W. Yu and J. G. Tobin, Phys. Rev. B **77**, 193409 (2008)
11. S.W. Yu, J.G. Tobin, and P. Söderlind**,** J. Phys. Cond. Matter **20**, 422202 (2008), Fast Track Communication; J.G. Tobin, J. Alloys Cmpds **444-445**, 154 (2007).
12. J.G. Tobin, S.W. Yu, B.W. Chung, G.D. Waddill, E. Damian, L. Duda and J. Nordgren, "Observation of Strong Resonant Behavior in the Inverse Photoelectron Spectroscopy of Ce Oxide," submitted to Phys. Rev B, 2010.
13. J.G. Tobin, P. Söderlind, A. Landa, K.T. Moore, A.J. Schwartz, B.W. Chung, M.A. Wall, J.M. Wills, R.G. Haire, and A.L. Kutepov, J. Phys. Cond. Matter **20**, 125204 (2008).
14. J.R. Naegele, "Actinides and Some of their Alloys and Compounds," Electronic Structure of Solids: Photoemission Spectra and Related Data, Landolt-Bornstein "Numerical Data and Functional Relationships in Science and Technology," ed. A Goldmann, Group III, Volume 23b, Pages 183 – 327 (1994); and references therein.
15. Y. Baer and J. Schoenes, Solid State Commun. **33**, 885 (1980), Y. Baer, Physica **102B**, 104 (1980).
16. G.C. Allen, I.R. Trickle and P.M. Tucker, Philos. Mag. B **43**, 689 (1981).
17. B.W. Veal and D.J. Lam, Phys. Rev. B **10**, 4902 (1974) and Phys. Letters **49A**, 466 (1974).

18. (A) E. Thibaut, J.J. Pireaux, J. Riga, C. Tenret-Noel, R. Caudano, E.G. Derouane, and J. Verbist, Proc. 2nd Int. Conf. Electron. Structure of the Actinides, eds. J. Mulak, W. Suski, and R. Troc, Wroclav, Poland, September 13 -16, 1976, p.139; (B) Gmelin Handbook of Inorganic Chemistry, 8th Edition, Supplement Vol. A5 ("Uranium"), Springer 1982, p 176.
19. J.J. Yeh and I. Lindau, Atomic Data and Nuclear Data Tables **32**, 99 (1985).
20. J.R. Naegele, J. Ghijsen and L. Manes, Actinides- Chemistry and Physical Properties, ed. L. Manes, Structure and Bonding, Vol 59/60, Berlin/Heidelberg, Springer, 1985, p 197.
21. S. Evans, J. Chem. Soc. Faraday Trans. 2, **73**, 1341 (1977).

Confirmation of Sample Quality: XPS and UPS of UO_2[a]

Figure captions

Figure 1a Schematic of BIS and spin resolved photoelectron spectroscopy (SRPES) experimental setup installed recently at Lawrence Livermore National Lab for the electronic structure study of actinides. For BIS, the detection of the photons is performed with the XES-350 monochromator and multi-channel detector

Figure 1b The Fano Spectroscopy results for Pt. The electrons were collected along the sample normal. The He I radiation was incident from either the left or the right side, at an angle of 45 degrees. The spin measured was perpendicular to the plane containing the He I radiation and the sample normal. (3A) The asymmetries from the left and right HeI sources, showing the spin reversal with chirality reversal. (3B) The polarization. (3C) The spin resolved and spin integrated spectra, using unpolarized HeI photons as the excitation. Spin up (down) is blue (red).

Figure 1c Prediction of the dichroism in δ-Pu. Double Polarization Photoelectron Dichroism is the ideal technique with which to probe for such a dynamically shielded moment, with (1) a probe time on the scale of 10^{-18} seconds and (2) the capability to see spin effects in nonmagnetic materials.

Figure 2 Wide scans with AlK-alpha and MgK-alpha. See text for details.

Figure 3 U4f spectra with AlK-alpha and MgK-alpha. See text for details.

Figure 4 O1s spectra with AlK-alpha and MgK-alpha. See text for details.

Figure 5 U4d spectra with AlK-alpha and MgK-alpha. See text for details.

Figure 6 XPS and UPS valence bands. See text for details.

Confirmation of Sample Quality: XPS and UPS of UO_2[a]

Figure 1a

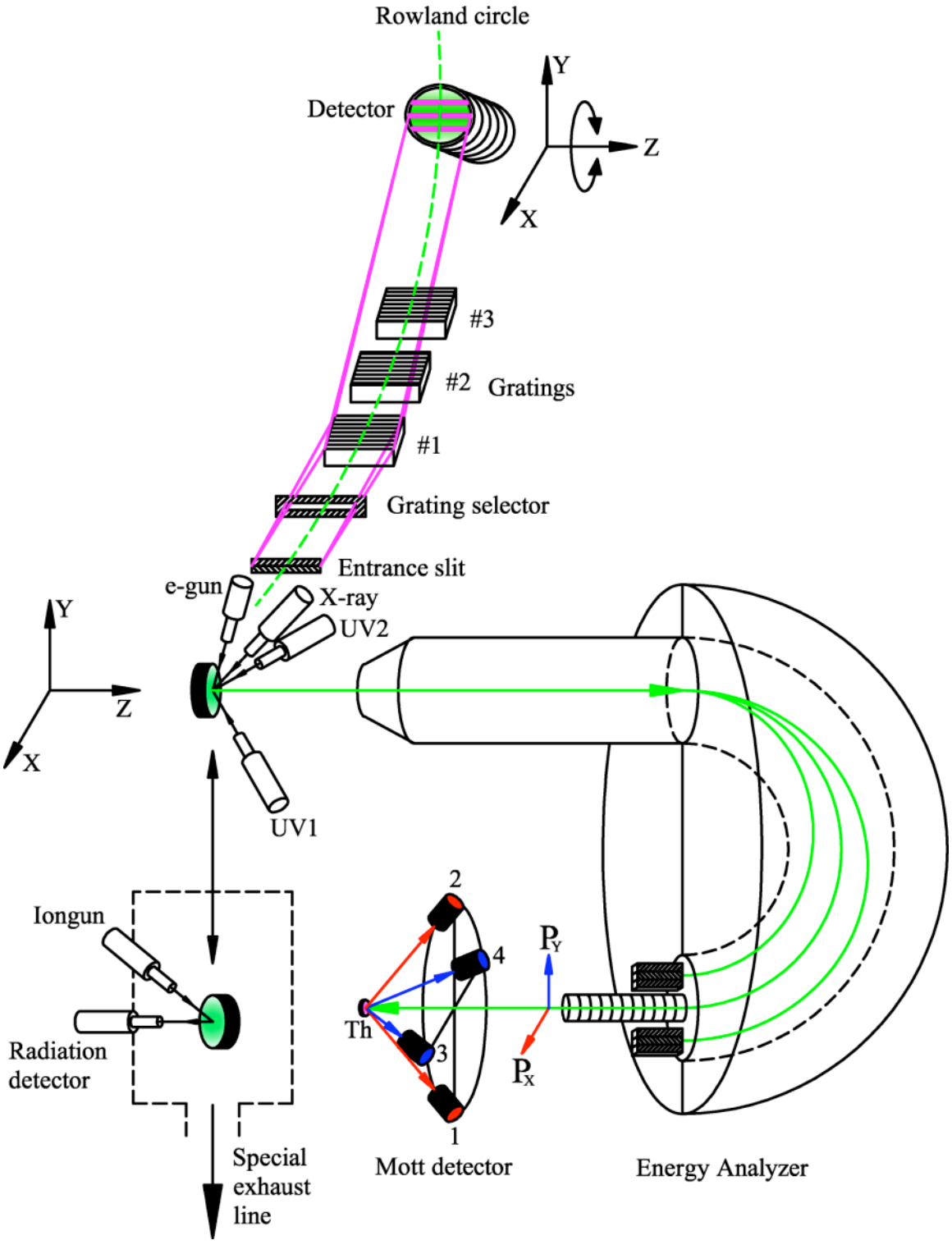

Confirmation of Sample Quality: XPS and UPS of UO_2[a]

Figure 1b

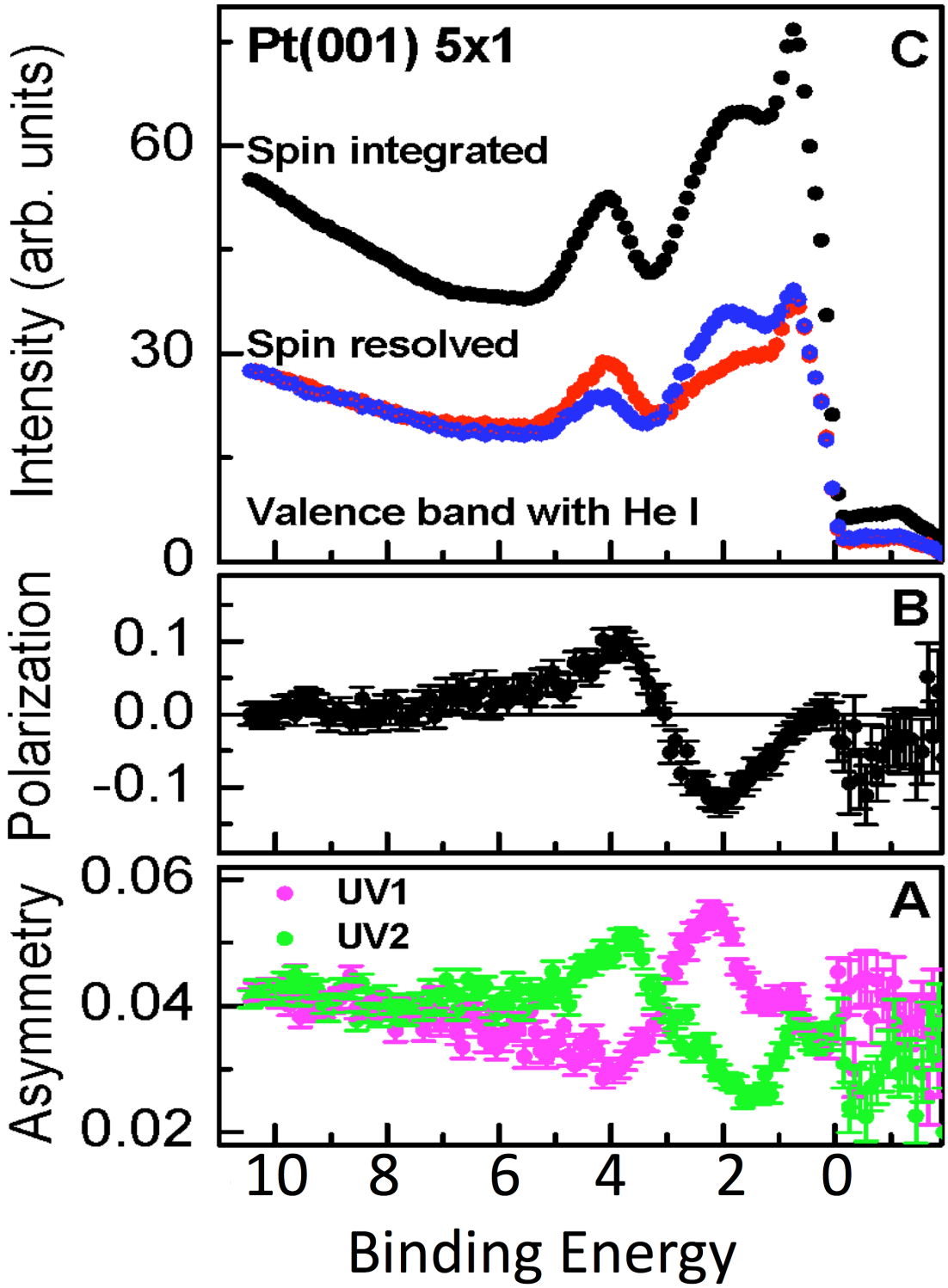

Confirmation of Sample Quality: XPS and UPS of UO_2[a]

Figure 1c

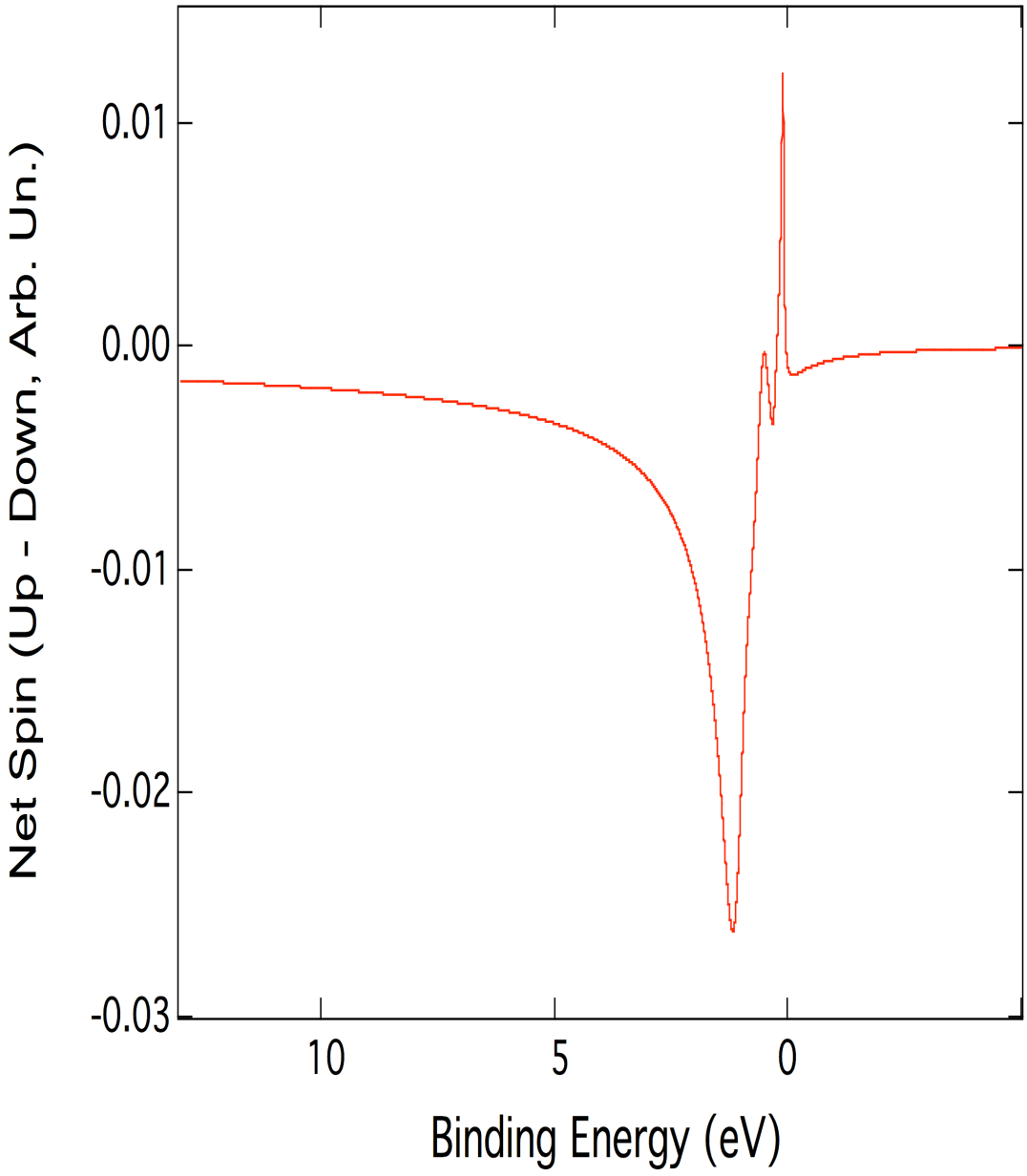

Confirmation of Sample Quality: XPS and UPS of UO_2[a]

Figure 2

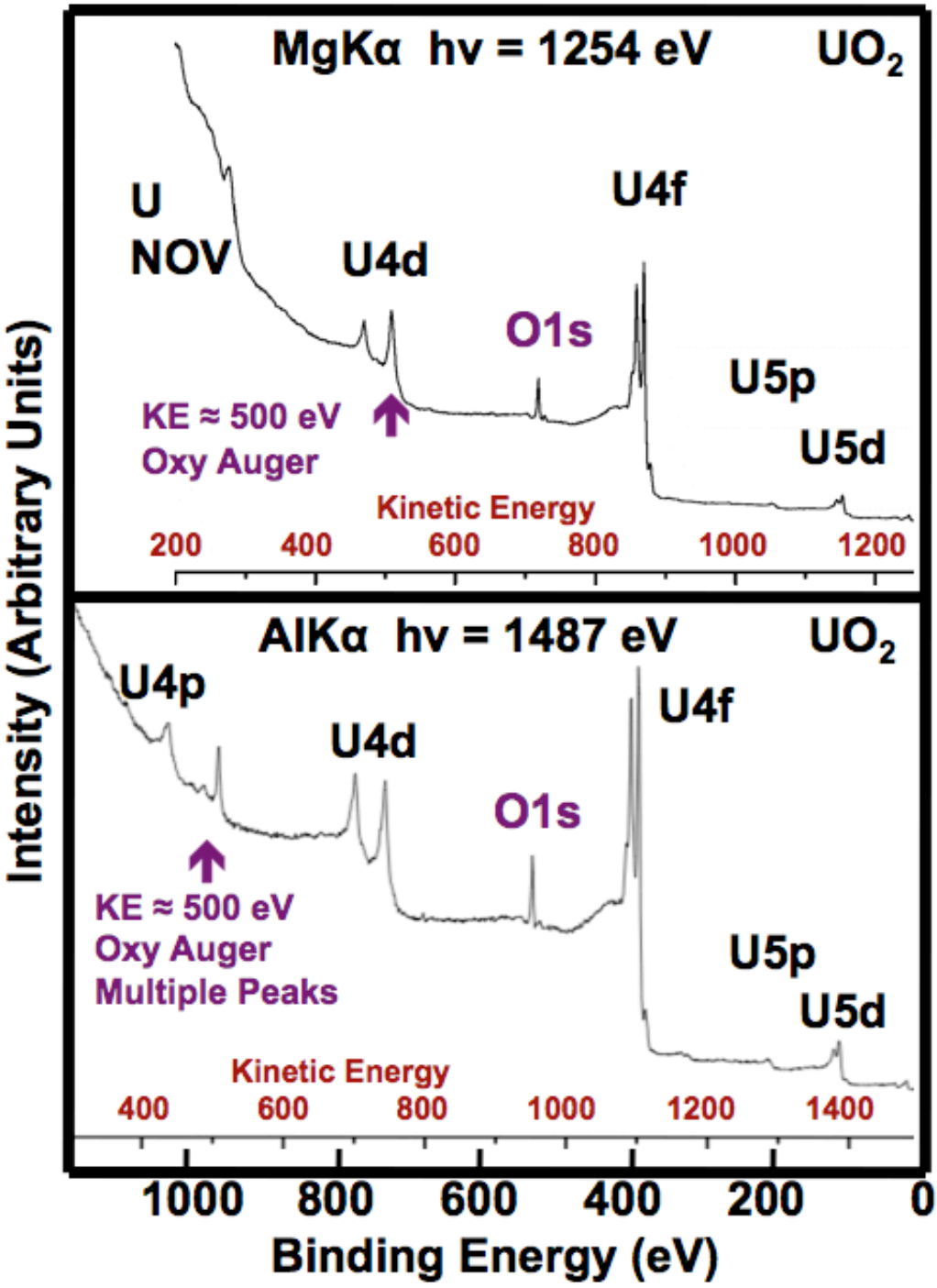

Confirmation of Sample Quality: XPS and UPS of UO_2[a]

Figure 3

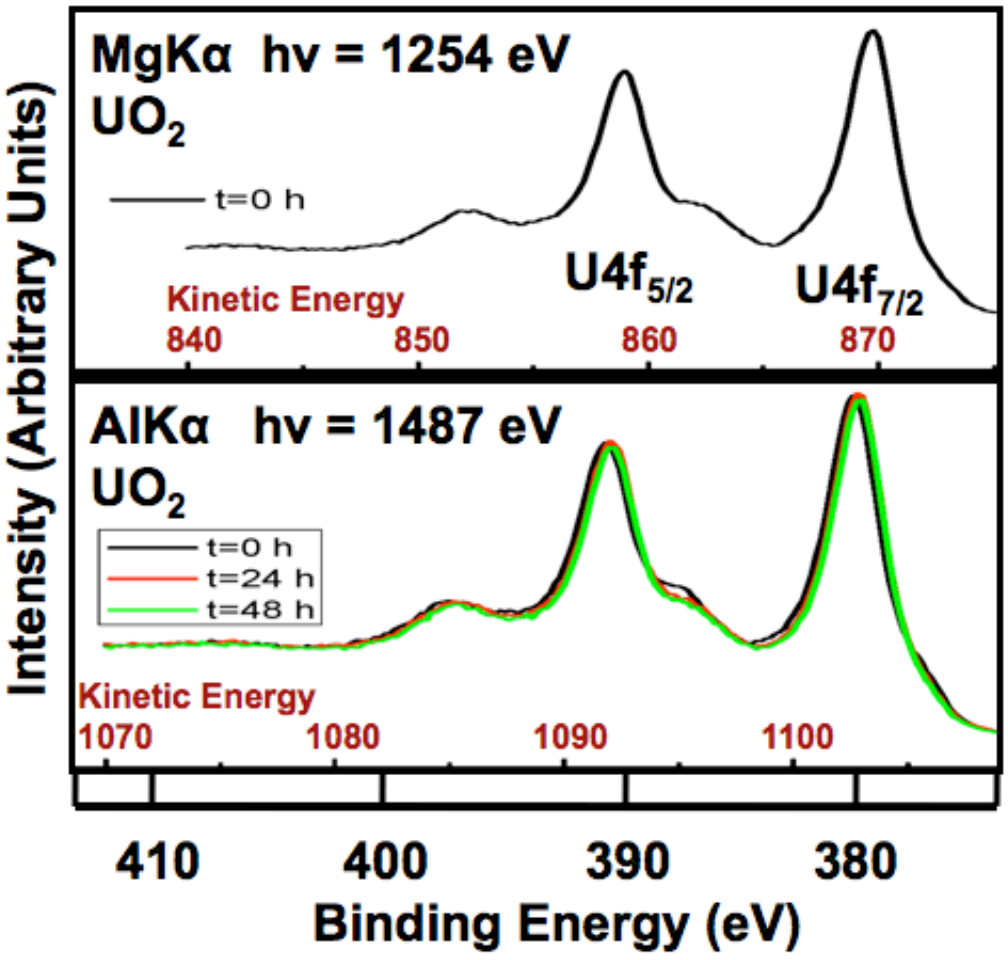

Confirmation of Sample Quality: XPS and UPS of UO_2[a]

Figure 4

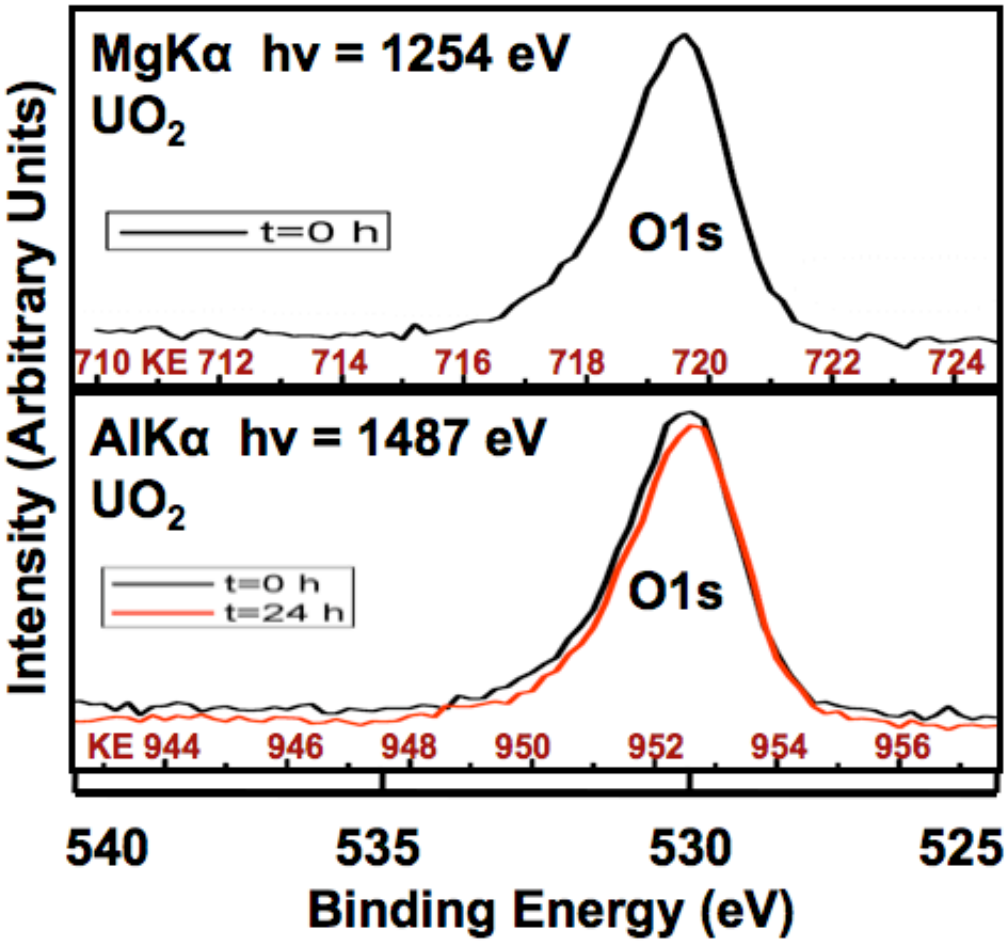

Confirmation of Sample Quality: XPS and UPS of UO_2[a]

Figure 5

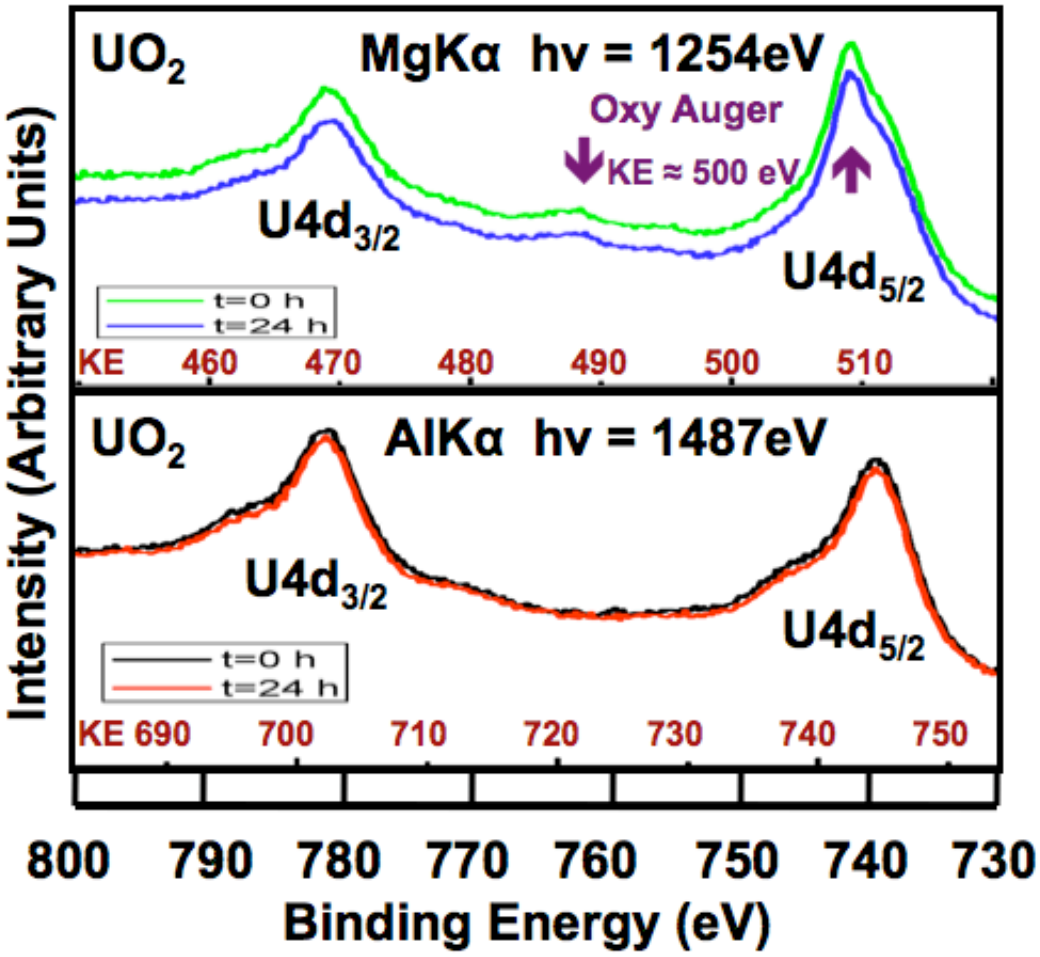

Confirmation of Sample Quality: XPS and UPS of UO_2[a]

Figure 6